

## Heavy neutral leptons at ANUBIS

Martin Hirsch<sup>1,\*</sup> and Zeren Simon Wang<sup>2,†</sup><sup>1</sup>*AHEP Group, Instituto de Física Corpuscular – CSIC/Universitat de València  
Calle Catedrático José Beltrán, 2 E-46980 Paterna, Spain*<sup>2</sup>*Asia Pacific Center for Theoretical Physics (APCTP) - Headquarters San 31,  
Hyoja-dong, Nam-gu, Pohang 790-784, Korea*

Recently Bauer *et al.* [1] proposed ANUBIS, an auxiliary detector to be installed in one of the shafts above the ATLAS or CMS interaction point, as a tool to search for long-lived particles. Here, we study the sensitivity of this proposal for long-lived heavy neutral leptons (HNLs) in both minimal and extended scenarios. We start with the minimal HNL model where both production and decay of the HNLs are mediated by active-sterile neutrino mixing, before studying the case of right-handed neutrinos in a left-right symmetric model. We then consider a  $U(1)_{B-L}$  extension of the Standard Model (SM). In this model HNLs are produced from the decays of the mostly SM-like Higgs boson, via mixing in the scalar sector of the theory. In all cases, we find that ANUBIS has sensitivity reach comparable to the proposed MATHUSLA detector. For the minimal HNL scenario, the contributions from  $W$ 's decaying to HNLs are more important at ANUBIS than at MATHUSLA, extending the sensitivity to slightly larger HNL masses at ANUBIS.

## I. INTRODUCTION

Recent years have seen a surge of interest in long-lived particles (LLPs), both from experimental and theoretical sides. Several new detectors have been proposed to search for LLPs using the LHC beams: MATHUSLA [2, 3], FASER [4–6], CODEX-b [7, 8] and AL3X [9, 10]. In addition, there is the SHiP proposal [11]. Different from all the other experiments mentioned above, however, SHiP is a beam-dump experiment. For a recent review on LLPs at the LHC see Ref. [12].<sup>1</sup>

Ref. [1] proposed a new far detector design called “AN Underground Belayed In-Shaft search experiment” (ANUBIS) to be constructed inside one of the shafts above either the ATLAS or CMS interaction point (IP) at the LHC. In this paper, we estimate the sensitivity reach of ANUBIS for heavy neutral leptons (HNLs) in various models and compare it with other proposed LLP far detectors.

From the theory point of view, LLPs appear in a variety of standard model (SM) extensions. Nowadays, in the literature very often dark matter motivated “Higgs portal” models are discussed as a motivation for LLPs. However, LLPs have a long history. For example several supersymmetric models, such as gauge mediated Supersymmetry (SUSY) breaking models and split SUSY, have

been known for quite some time to predict LLPs; for a recent review see Ref. [14]. We would also like to mention explicitly bilinear R-parity breaking SUSY, where it has been shown that the lifetime of the LLP is correlated with the small neutrino masses [15].

The observation of neutrino oscillations has firmly established that neutrinos have non-zero mass. (For the experimental status of neutrino data, see for example Refs. [16, 17].) Many different models have been proposed to understand the small neutrino masses. The simplest is the well-known type-I seesaw [18–22]. Here, neutral leptons are added to the SM particle content. These HNLs mix with the ordinary neutrinos after electroweak symmetry breaking, typically  $V_{\alpha N} \propto (Y_{\alpha N}^\nu v)/m_N$ , with the light neutrino mass given by the famous seesaw relation:  $m_\nu \propto (Y^\nu v)^2/m_N$ . The decay width of these HNLs are suppressed by  $|V_{\alpha N}|^2$ , leading automatically to very long-lived HNLs, if their mass is below the electroweak scale.<sup>2</sup>

In the simplest HNL model both production cross section and decay width are proportional to  $|V_{\alpha N}|^2$ . However, there are a number of SM extensions, which give much larger HNL production cross sections, while still maintaining very long decay lengths. We will estimate ANUBIS's sensitivity for two of these: (i) the minimal left-right symmetric model (LRSM) [24–26] and (ii) the SM extended by an additional  $U(1)_{B-L}$  group. For the latter we use the model variant discussed in some other

\* mahirsch@ific.uv.es

† zerenSimon.wang@apctp.org

<sup>1</sup> A study of potential far detectors at future lepton colliders was performed in Ref. [13].<sup>2</sup> The mixing between sterile and active neutrinos can be larger in non-minimal seesaw models such as the inverse seesaw [23].

recent papers studying LLPs [27–29]. In all three model variants we find that ANUBIS has sensitivity reach comparable to the proposed MATHUSLA detector.

In the following section, we will introduce the different models with HNLs. Sec. III is devoted to describing the detector setup and the details of the simulation. In Sec. IV we present the numerical results. We conclude and summarize our findings in Sec. V.

## II. MODEL BASICS

### A. The minimal HNL scenario

The minimal HNL model adds  $n$  species of HNLs to the particle content of the SM. They enter both charged-current (CC) and neutral-current (NC) interactions, suppressed compared to the SM electroweak coupling strength by small mixing parameters:

$$\mathcal{L} = \frac{g}{\sqrt{2}} V_{\alpha N_j} \bar{\ell}_\alpha \gamma^\mu P_L N_j W_{L\mu}^- + \frac{g}{2 \cos \theta_W} \sum_{\alpha, i, j} V_{\alpha i}^L V_{\alpha N_j}^* \bar{N}_j \gamma^\mu P_L \nu_i Z_\mu, \quad (1)$$

where  $i = 1, 2, 3$ ,  $j = 1, \dots, n$ , and  $\ell_\alpha$  ( $\alpha = e, \mu, \tau$ ) are the charged leptons of the SM.  $V_{\alpha N_j}$  labels the mixing between SM light neutrinos and the HNLs of mass  $m_{N_j}$ . By  $V_{\alpha i}^L$  we denote the mixing within the active neutrino sector, in the basis where the charged lepton mass matrix is diagonal. With this choice of basis, the elements of  $V_{\alpha i}^L$  corresponds to the mixing angles measured in oscillation experiments.

Neutrino data requires that  $n \geq 2$ . However, for simplicity we assume that there is only one species of the HNL,  $N$ , light enough to be produced at the LHC. We treat  $V_{\alpha N}$  as a free parameter, to be determined experimentally, and calculate the total decay width of the HNL using the analytical formulas given in Ref. [30]. Such HNLs are most dominantly produced from on-shell decays of various kinds of SM particles at the LHC. For this minimal HNL scenario, we take into account different production channels:  $D$ -mesons,  $B$ -mesons,  $W$ -bosons,  $Z$ -bosons, SM Higgs bosons  $h$ , and the top quark  $t$ . For the mesons channels, we include into the calculation both three-body and two-body decays. Note that there is a recent study on the sensitivity of future experiments for three-body decays of mesons [31].

### B. The minimal left-right symmetric model

We consider the minimal left-right symmetric model which has gauge group  $SU(3)_C \times SU(2)_L \times SU(2)_R \times U(1)_{B-L}$  [24, 25]. Right-handed neutrinos are necessarily present in this model in the right-handed lepton doublet. Breaking the left-right symmetry group to the SM group via a right triplet scalar generates Majorana masses for the right-handed neutrinos and thus automatically a see-saw mechanism [26].

The CC and NC interactions relevant for our analysis are

$$\mathcal{L} = \frac{g_R}{\sqrt{2}} (\bar{d} \gamma^\mu P_R u + V_{\alpha N}^R \cdot \bar{l}_\alpha \gamma^\mu P_R N) W_{R\mu}^- + \frac{g_R}{\sqrt{1 - \tan^2 \theta_W (g_L/g_R)^2}} \times Z_{LR\mu}^\mu \bar{f} \gamma_\mu [T_{3R} + \tan^2 \theta_W (g_L/g_R)^2 (T_{3L} - Q)] f \quad (2)$$

where  $V_{\alpha N}^R$  is the right-handed sector neutrino mixing matrix. Different from  $V_{\alpha N}$  describing left-right mixing, one expects that the entries of  $V_{\alpha N}^R$  are  $\mathcal{O}(1)$ . The charged  $W_{L,R}$ -boson states can be expressed in terms of the mass eigenstates, by a mixing angle  $\zeta$ . Since  $\zeta \ll 1$ , for simplicity we will call the  $W$ -bosons  $W_{L,R}$ , instead of the more correct (but somewhat awkward)  $W_{1,2}$ .

For the production of the right-handed neutrinos at the LHC in this model, there are different contributions. First, there is the on-shell production of  $W_R$ , with the  $W_R$  decaying to  $N + l_\alpha$ . Second,  $N$  can appear in the decays of mesons, through the decays of off-shell  $W_L$ , suppressed by the small active-sterile neutrino mixing  $V_{\alpha N}$ . And, finally, mesons can decay via off-shell  $W_R$  to  $N$  plus charged leptons<sup>3</sup>. Relative to the off-shell  $W_L$  contribution, the off-shell  $W_R$  contribution then can be estimated via  $|V_{\alpha N}|^2 \rightarrow |V_{\alpha N}^R|^2 (g_R/g_L)^4 (m_{W_L}/m_{W_R})^4$ . For our sensitivity estimates, we assume that  $|V_{\alpha N}|^2$  is given by the naive seesaw estimate and, thus, small enough that the  $N$  production from meson decays and the decay width of  $N$  are dominated by the off-shell  $W_R$  contribution. Note, that contributions to  $N$  decay from off-shell  $Z_R$  are completely negligible in this approximation.

We will again focus on the case with only one right-handed neutrino  $N$  within the kinematic region of interest ( $m_N \lesssim m_B$ ). We will use  $g_L/g_R = 1$  in our numerical study, the results can be easily scaled to other values of  $g_R$ .

<sup>3</sup> See Ref. [32] for an earlier study on the sensitivity of meson decays in the LRSM at a number of future searches.

### C. HNLs in $U(1)_{B-L}$

One of the simplest SM extensions automatically predicting HNLs is adding a gauged  $U(1)_{B-L}$  to the SM gauge group [33, 34]. The model variant we will be using in our numerical estimate and its implications for accelerator searches has been discussed recently in Refs. [27, 28, 35–37]. Apart from the HNLs, the model predicts a  $Z'$  and (at least) a second Higgs. This new scalar, required to break  $U(1)_{B-L}$ , will mix with the (mostly) SM Higgs, observed at the LHC, via a small mixing angle  $\beta$ .

Two new channels for producing HNLs, besides the standard active-sterile neutrino mixing, then exist in this model. First, HNLs can be pair produced from a light  $Z'$  decay [28], or, second, the SM-like Higgs will decay through mixing to a pair of HNLs [27, 35]. In our numerical calculation, we choose to concentrate on the SM-like Higgs decay channel. The decay width of the HNLs to SM particles in this model again is proportional to the mixing  $|V_{\alpha N}|^2$ .

We choose the benchmark values for the model parameters, following the discussion and choices in Refs. [27, 38]:

$$\begin{aligned} m_N &= 1 - 60 \text{ GeV}, V_{\alpha N} = 10^{-9} - 10^{-2}, \\ m_{Z'} &= 6 \text{ TeV}, g'_1 = 0.8, \tilde{x} = 3.75 \text{ TeV}, \\ m_H &= 450 \text{ GeV}, \sin \beta = 0.3, \end{aligned} \quad (3)$$

where  $\tilde{x} = m_{Z'}/2g'_1$  is the VEV of the extra scalar,  $\beta$  is the scalar mixing angle, and  $m_H$  is the mass of the heavier scalar. (The latter does not affect our calculation directly.) Ref. [38] derived current lower (upper) limits on  $m_{Z'}$  ( $g'_1$ ) by recasting the ATLAS and CMS searches [39, 40]. As for the latest bounds on  $m_H$  and  $\sin \beta$ , one may refer to Ref. [29].

The decay width of the SM-like Higgs into a pair of HNLs for one single generation is [35]:

$$\Gamma(h \rightarrow NN) = \frac{1}{2} \frac{m_N^2}{\tilde{x}^2} \sin^2 \beta \frac{m_h}{8\pi} \left(1 - \frac{4m_N^2}{m_h^2}\right)^{3/2}, \quad (4)$$

where we assume that among the three generations of HNLs predicted, only one generation labelled with  $N$  is below the Higgs decay threshold:  $m_N < m_h/2$ .

The decay branching ratio of the SM-like Higgs bosons into a pair of HNLs can then be written as:

$$\text{Br}(h \rightarrow NN) = \frac{\Gamma(h \rightarrow NN)}{\Gamma(h \rightarrow NN) + \cos^2 \beta \Gamma_{\text{SM}}^h}, \quad (5)$$

where  $\Gamma_{\text{SM}}^h = 4.1 \text{ MeV}$  [41] is the SM Higgs total decay width for  $m_h = 125.10 \text{ GeV}$ .

Production cross section for a pair of  $N$ 's is expressed with the following formula:

$$\sigma(pp \rightarrow h \rightarrow NN) = \cos^2 \beta \cdot \sigma(pp \rightarrow h)_{\text{SM}} \cdot \text{Br}(h \rightarrow NN), \quad (6)$$

where the SM production cross section of the Higgs boson is modified by a factor  $\cos^2 \beta$  and  $\text{Br}(h \rightarrow NN)$  is calculated with Eq. (5).

### III. DETECTOR SETUP & SIMULATION

Fig. 1 shows two profile sketches of the ANUBIS detector setup in the  $y-z$  and  $x-z$  planes, respectively, where the collider beams are oriented along the  $z$ -direction. The cylindrical detector is horizontally (vertically) displaced from the IP with a distance  $d_h = 5$  ( $d_v = 24$ ) m. It has a length of  $l_v = 56$  m and a diameter  $l_h = 18$  m. With four tracking stations, the detector may be divided into three segments with the length of each segment  $l_v^{\text{seg}}$  roughly equal to 18.7 m. We label the polar angle of a sample long-lived  $N_i$  with  $\theta_i$ .

The total number of HNLs produced is calculated with

$$n_N = n_M \cdot \text{Br}(M \rightarrow nN) \cdot n, \quad (7)$$

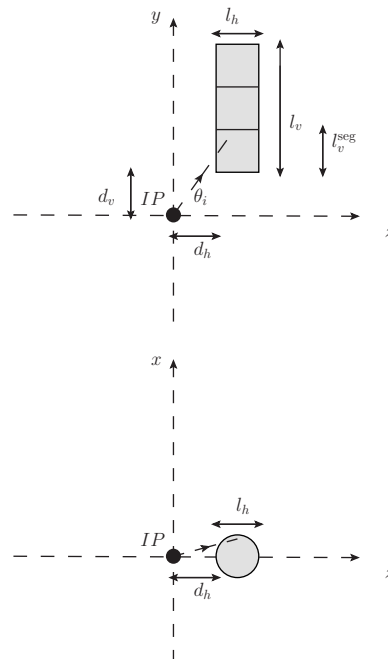


FIG. 1. Profile sketches of the ANUBIS detector in the  $y-z$  and  $x-z$  planes, respectively. In the upper plot we depict a sample long-lived HNL by the arrowed dashed line with  $\theta_i$  labeling its polar angle.

$M$	$b\bar{b}$	$c\bar{c}$	$h$	$t\bar{t}$	$W$	$Z$
$\sigma_M$ [pb]	$6 \times 10^8$	$2 \times 10^{10}$	$6 \times 10^1$	$1 \times 10^3$	$2.1 \times 10^5$	$6.4 \times 10^4$

TABLE I. (Rough) production cross section of each type of mother particles of the HNLs at LHC with  $\sqrt{s} = 14$  TeV. For  $c\bar{c}$  we take into account all of  $D^0$ ,  $D^+$ ,  $D_s$ , and  $D^{0*}$  mesons. For references see text.

where  $n_M$  stands for the total number of a mother particle  $M$  produced. For high-luminosity LHC's integrated luminosity  $\mathcal{L}_{\text{int}} = 3 \text{ ab}^{-1}$  and the center-of-mass energy  $\sqrt{s} = 14$  TeV,  $n_M = \mathcal{L}_{\text{int}} \cdot \sigma_M$  for  $M = h, W$ , and  $Z$ , and twice that for  $M$  being  $D$ -mesons,  $B$ -mesons, and top quarks, since the latter are mainly pair-produced at the LHC.  $\sigma_M$  denotes the production cross section of each channel, and  $\text{Br}(M \rightarrow nN)$  labels the decay branching ratio of  $M$  into  $n$   $N$ 's ( $n = 1, 2, \dots$ ). In Table I, we list the production cross section over a whole sphere for each channel at the LHC for  $\sqrt{s} = 14$  TeV. We follow the procedure explained in Ref. [42] to obtain  $\sigma_M$  for  $D$ -,  $B$ -mesons,  $W$ -bosons, and  $Z$ -bosons at  $\sqrt{s} = 13$  TeV. We then rely on the Monte-Carlo (MC) simulation tool `Pythia 8.243` [43, 44] to extrapolate the cross section to  $\sqrt{s} = 14$  TeV. Slightly depending on the production channel, cross sections are changed by roughly a factor  $\sim 1.07$  by this change of  $\sqrt{s}$ . As for the production cross section of  $h$  and  $t\bar{t}$ , we extract the numbers from Refs. [45, 46].

We express the total number of visible displaced vertices inside the ANUBIS as a function of  $n_N$ , average decay probability inside the fiducial volume  $\langle P[N \text{ in f.v.}] \rangle$ , and the decay branching ratio of the HNLs into visible states (we include all the decay channels except the completely invisible tri-neutrino one):

$$n_N^{\text{vis}} = n_N \cdot \langle P[N \text{ in f.v.}] \rangle \cdot \text{Br}(N \rightarrow \text{visible}), \quad (8)$$

where  $\langle P[N \text{ in f.v.}] \rangle$  is estimated by performing MC simulation with `Pythia 8`:

$$\langle P[N \text{ in f.v.}] \rangle = \frac{1}{n_N^{\text{MC}}} \sum_{i=1}^{n_N^{\text{MC}}} P[N_i \text{ in f.v.}]. \quad (9)$$

$n_N^{\text{MC}}$  labels the total number of MC-simulated  $N$ 's and  $P[N_i \text{ in f.v.}]$  denotes the individual decay probability of each simulated  $N$  taking into account the detector geometry of ANUBIS and the kinematics of the HNLs. To evaluate  $P[N_i \text{ in f.v.}]$ , we divide the ANUBIS decay volume into three segments corresponding to its 4 equally spaced tracking stations and add up the decay probab-

ilities inside each segment:

$$P[N_i \text{ in f.v.}] = \sum_{j=1}^3 \frac{\delta\phi^j}{2\pi} \cdot e^{-\frac{L_i^j}{\lambda_i^z}} \cdot (1 - e^{-\frac{L_i^{j'}}{\lambda_i^z}}), \quad (10)$$

$$\delta\phi^j = 2 \arctan \frac{l_h/2}{d_v + (2j-1)/2 \cdot l_v^{\text{seg}}}, \quad (11)$$

$$L_i^j = \min \left( \max \left( d_h, \frac{d_v + (j-1) \cdot l_v^{\text{seg}}}{\tan \theta_i} \right), d_h + l_h \right), \quad (12)$$

$$L_i^{j'} = \min \left( \max \left( d_h, \frac{d_v + j \cdot l_v^{\text{seg}}}{\tan \theta_i} \right), d_h + l_h \right) - L_i^j, \quad (13)$$

$$\lambda_i^z = \beta_i^z \gamma_i c \tau. \quad (14)$$

Eq. (14) calculates the boosted decay length of the  $i$ -th simulated  $N$  along the beam direction, making use of its speed in the longitudinal direction  $\beta_i^z$ , boost factor  $\gamma$ , and proper lifetime  $\tau$  with  $c$  denoting the speed of light. The speed and boost factor can be easily obtained from kinematic information of the HNLs provided in `Pythia 8`:

$$\beta_i^z = |p_i^z/E|, \quad \gamma_i = E_i/m_N, \quad (15)$$

where  $p_i^z$  is the momentum along the  $z$ -direction, and  $E_i$  is the energy. For the azimuthal angle coverage we choose the middle position of each segment in order to fix the reference height.

We simulate 100k events for each parameter point using `Pythia 8`. In order to obtain the maximal number of statistics, we require the mother particles to exclusively decay in the channels leading to HNL production. We then calculate the decay branching ratios of the mother particles into HNLs analytically.

We cross-checked the usage of Eq. (10) by including  $N$ 's decay in `Pythia 8` and simulating 10 million events and compared the sensitivity plots of both approaches. This method is very time-consuming and does not lead to smooth sensitivity curves even with 10 million MC events. However, overall both calculations lead to similar final results.

## IV. RESULTS

We present numerical results in this section. As discussed in Ref. [1], ANUBIS should be a nearly background-free experiment. Backgrounds from cosmic rays should be negligible as a result of directional cuts. A more important background source could be long-lived neutral SM particles, such as  $K_L^0$ , which might reach

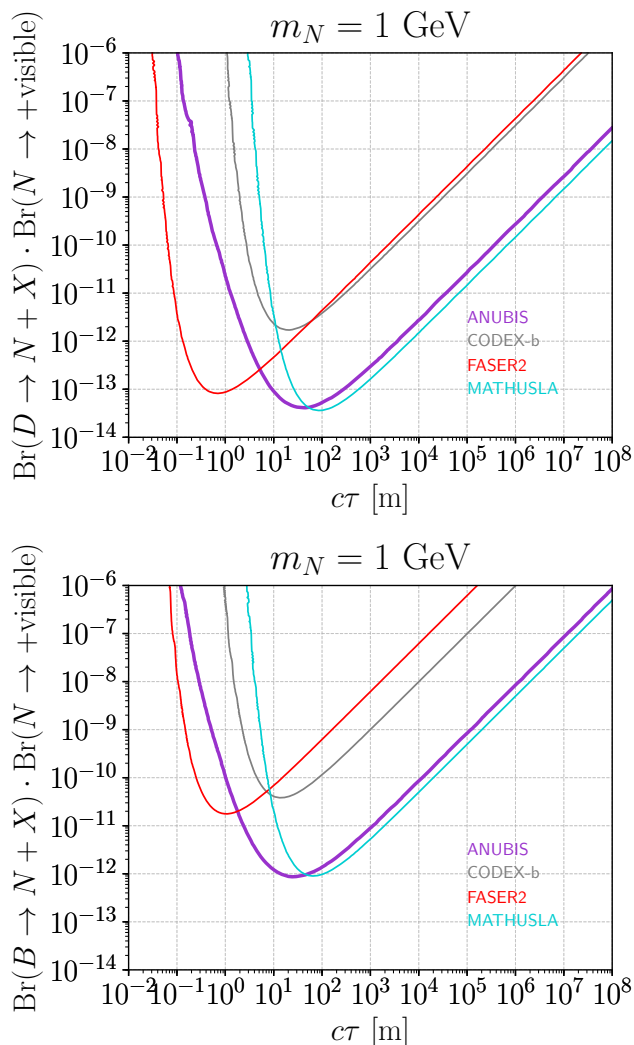


FIG. 2. The sensitivity estimates for ANUBIS, compared with MATHUSLA, CODEX-b and FASER2, in the plane branching ratio versus  $c\tau$ , for HNLs from  $D$ -decays (upper plot) and  $B$ -decays (lower plot), in the context of the minimal HNL scenario.

ANUBIS and decay within the detector volume. Ref. [1] proposes to use the ATLAS calorimeter as an active veto to eliminate this background. In our figures below we always show the 3-events sensitivity lines for ANUBIS. In case zero background can be reached, these lines correspond to 95% C.L. (confidence level) limits.

### A. Sensitivities for different production modes

In Fig. 2 we present sensitivity estimates for ANUBIS for a long-lived neutral fermion of mass 1 GeV, produced from  $D$ - and  $B$ -mesons decays, using the minimal HNLs as the benchmark model. The two plots in the fig-

ure show the plane  $\text{Br}(D/B \rightarrow N + X) \cdot \text{Br}(N \rightarrow \text{visible})$  vs.  $c\tau$ , where  $c\tau$  is the proper decay length of  $N$ , and  $\text{Br}(N \rightarrow \text{visible}) \approx 91.2\%$  for  $m_N = 1$  GeV.

The exclusion-limit isocurves for CODEX-b ( $300 \text{ fb}^{-1}$ ), FASER2 ( $3 \text{ ab}^{-1}$ ), and MATHUSLA ( $3 \text{ ab}^{-1}$ ) are reproduced from Ref. [42]<sup>4</sup>. As the figure shows, for both  $B$ - and  $D$ -decays the minimum branching ratios that can be explored are very similar for ANUBIS and MATHUSLA, despite ANUBIS having a much smaller instrumented volume. This can be simply traced to the much smaller distance of ANUBIS from the IP. As a result of this and of the fact that the HNLs of mass 1 GeV traveling inside the window of MATHUSLA typically have boost factors larger than those of the HNLs traveling towards ANUBIS by less than a factor 2, relative to ANUBIS, MATHUSLA’s maximal sensitivity occurs at larger values of  $c\tau$ . Compared to FASER2 and CODEX-b, ANUBIS shows clearly better sensitivity. Note that the huge change in FASER2’s sensitivity relative to the other experiments, when going from  $B$ - to  $D$ -meson decays. This is caused by the very forward position of FASER2, with lighter particles produced more forward at the LHC. Recall, that CODEX-b is supposed to have only  $10^3 \text{ m}^3$  of decay volume, with FASER being even smaller, while ANUBIS will have roughly  $1.5 \times 10^4 \text{ m}^3$  of volume.

We also comment on the usage of the mean value of  $\beta \cdot \gamma$  for calculating the decay probability in Ref. [42]. For large  $c\tau$  in the linear regime, this choice is a good approximation. However, for small values of  $c\tau$ , the tail of the  $\beta \cdot \gamma$  distribution has a dominant contribution to the decay probability, and thus using the average  $\beta \cdot \gamma$  underestimates the reach in the decay branching ratios of the mesons into HNLs.

### B. Results- the minimal scenario and the LRSM

We show the results for the minimal model of HNLs in Fig. 3 in the plane  $|V_{\alpha N}|^2$  vs.  $m_N$ , where we con-

<sup>4</sup> The setup of “FASER<sup>R</sup>” considered in Ref. [42] is only slightly different from the approved configuration of FASER2 described in Ref. [47], and the final results should be similar. During the completion of this work, we noticed that when we produced the plots in Fig. 1 of Ref. [42], we mistakenly failed to absorb the phase space suppression factor for a massive HNL into  $\text{Br}(B(D) \rightarrow N + X)$ , leading to a reduction of a factor  $\sim 2$  (10) in  $\text{Br}(B(D) \rightarrow N + X)$  reach for the left (right) plot of Fig. 1 in Ref. [42]. This computational mistake has been corrected here and the curves are updated in Fig. 2. The final results of Ref. [42] are unaffected by this error.

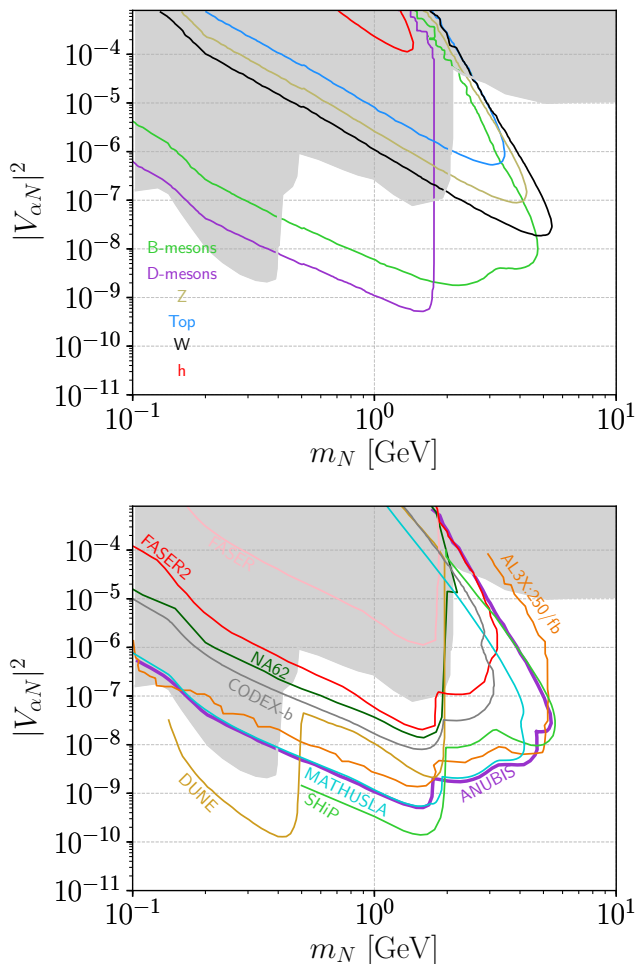


FIG. 3. The sensitivity reach of ANUBIS for HNLs produced from different channels (upper figure) and reach compared to other future experiments (lower figure), in the context of the minimal HNL scenario, with one generation of  $N$  mixing with  $\nu_\alpha$ ,  $\alpha = e/\mu$ .

sider one generation of  $N$  mixing with either  $\nu_e$  or  $\nu_\mu$  but not both ( $\alpha = e/\mu$ ). The upper plot compares the exclusion limits among different production channels at ANUBIS, while the lower compares combined sensitivities of the dominant production modes:  $B$ -,  $D$ -mesons, and  $W$ -bosons at ANUBIS with the limits at other future experiments. We show in the gray area in the background the experimentally excluded region of the parameter space based on the summary given in Ref. [48], including the searches from CHARM [49], PS191 [50], JINR [51], and DELPHI [52]. For the other future experiments, we extract the sensitivity projections from a series of past studies [6, 10, 42, 53–55]. Note that for the sensitivity prediction of DUNE extracted from Ref. [53], we only show the results for the HNLs mixing with the elec-

tron neutrinos. For the muon mixing case, the sensitivity limits only get reduced at roughly two mass thresholds  $m_K - m_\mu \sim 400$  MeV and  $m_D - m_\mu \sim 1800$  MeV, compared to the case where the electron mixing is dominant. Therefore, in order to keep the plot clean, we refrain from showing the muon mixing sensitivity curve for DUNE.

The comparison among different production modes shows that the heavy meson decays into HNLs have the strongest reach in  $|V_{\alpha N}|^2$  at  $\mathcal{O}(10^{-9})$  ( $5 \times 10^{-10}$ ) for  $m_N \lesssim 4$  ( $\sim 1.7$ ) GeV, and that the  $W$ -channel ( $W^+ \rightarrow e^+/\mu^+ N$ ) extends the mass reach to almost  $m_N = 6$  GeV for mixing squared of  $\sim 2 \times 10^{-8}$ . Compared to these channels, the Higgs bosons ( $h \rightarrow N\nu_\alpha$ ), top quarks ( $t \rightarrow W^+ b$ ,  $W^+ \rightarrow e^+/\mu^+ N$ ), and  $Z$ -bosons ( $Z \rightarrow N\nu_\alpha$ ) would have more limited contributions.

The lower plot of Fig. 3 compares the different future experiments' sensitivities on minimal HNLs. The exclusion limits of ANUBIS are comparable to that of MATHUSLA for  $m_N \lesssim 4$  GeV, and show the advantage for  $m_N$  slightly larger than 4 GeV by virtue of its better acceptance for HNLs produced from  $W$ -bosons decays, where MATHUSLA loses sensitivity.

The plots shown in Fig. 3 are valid for  $\alpha = e, \mu$ , assuming that the efficiencies for electrons and muons in ANUBIS are at least approximately equal. We also want to comment briefly on possible constraints on  $V_{\tau N}$ . Ref. [1] does not contain any information on detection efficiencies for  $\tau$ 's. Thus, we can not give definite predictions for  $V_{\tau N}$ . However, a few qualitative comments might be in order. Both of ANUBIS and MATHUSLA are sparsely instrumented, large-volume tracking detectors. In both experiments, muons will show up as single tracks, while taus will give either one or three collimated tracks. A discussion of tau detection in MATHUSLA can be found in Ref. [56]. The HNLs sensitivity curves for  $V_{\mu N}$  and  $V_{\tau N}$  shown in Ref. [3] allow us to estimate the sensitivity loss for MATHUSLA for the case of taus, to be in the order of (30–50) for mixing squared, depending on HNL mass. Given the similarities in the detector principles, it may not be unreasonable to suppose that the numbers for ANUBIS should be of a similar order. However, without more concrete input from the experimental side, we are unable to make more definite predictions in this paper.

For the HNLs produced from  $B$ - and  $D$ -mesons decays via an off-shell  $W_R$  at ANUBIS, we may re-interpret the corresponding results in the context of the minimal left-right symmetric model, by making the simple substitution  $|V_{\alpha N}|^2 \rightarrow (m_{W_L}/m_{W_R})^4$ , since we assume  $V_{\alpha N}^R \sim \mathcal{O}(1)$  and  $g_L/g_R = 1$ , as discussed in Sec. II. We perform the same substitution on the HNL sensitivities

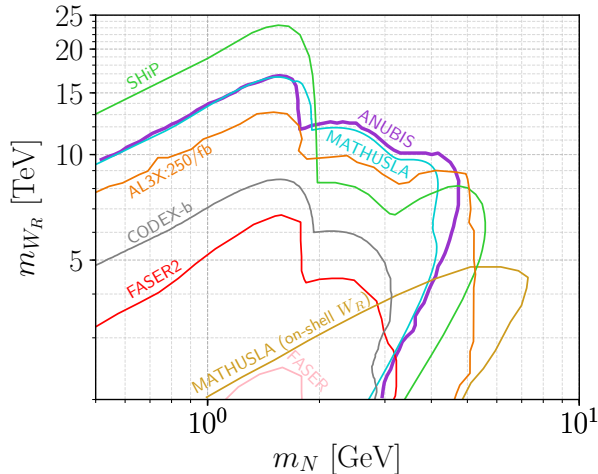


FIG. 4. The sensitivity reach of ANUBIS compared with other future experiments in the context of the minimal left-right symmetric model. All the curves are for HNLs produced from bottom and charm mesons decays except one MATHUSLA limit on the lower right which is for on-shell  $W_R$  decays.

of SHiP, MATHUSLA, AL3X, CODEX-b, FASER, and FASER2 as well, as their physics reaches are also dominated by the mesons channels. We refrain from showing the ATLAS expectations as they are sensitive to larger values of  $m_N$ . We further extract the MATHUSLA sensitivity for on-shell  $W_R$  decays at the HL-LHC from Ref. [3] considering the Keung-Sejanović process [57]. The results are presented in Fig. 4 in the plane  $m_{W_R}$  vs.  $m_N$ . We find that for  $m_N$  below the bottom meson threshold the heavy meson decays to HNLs provide the strongest probe for  $m_{W_R}$ , while the limits coming from on-shell  $W_R$ 's are restricted to  $m_{W_R} \leq 5$  TeV.

### C. Results-HNLs from SM-like Higgs decays in $U(1)_{B-L}$ model

We present the results for another non-minimal HNL scenario with a new  $U(1)_{B-L}$  gauge group and focus on the SM-like Higgs decay into a pair of HNLs which mix with  $\nu_{e/\mu}$ . With the selected benchmark parameters given in Eq. (3), we obtain the sensitivities in the plane  $|V_{\alpha N}|^2$  vs.  $m_N$ , shown in Fig. 5. The gray band indicates the interesting area of the parameter space corresponding to the type-I seesaw limits for light neutrino masses between 0.01 eV and 0.3 eV. The calculation of the decay probability of HNLs inside MATHUSLA follows from applying the formulas given in Ref. [58] for the 200 m  $\times$  200 m  $\times$  20 m setup. We find that for  $m_N$  between 5 (6) GeV

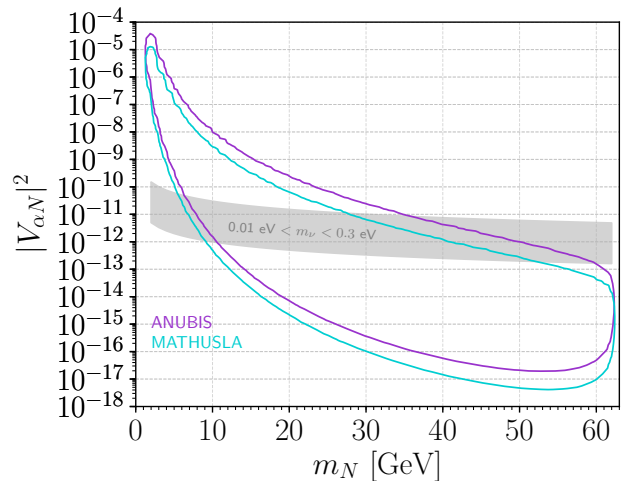


FIG. 5. The sensitivity reaches of ANUBIS and MATHUSLA for HNLs produced from the SM-like Higgs decays in the context of the  $U(1)_{B-L}$  model.

and 52 (60) GeV, MATHUSLA (ANUBIS) may probe the type-I seesaw limits on  $|V_{\alpha N}|^2$  for the considered range of  $m_\nu$ . Though the two detectors show similar sensitivity reaches, compared to MATHUSLA ANUBIS is sensitive to slightly larger values of  $|V_{\alpha N}|^2$  mainly because of its shorter distance from the IP. The sensitive area in the parameter space presented here may shrink if in the future the experimental upper (lower) bound on the scalar mixing angle  $\beta$  (scalar VEV  $\tilde{x}$ ) gets more constrained.

## V. CONCLUSIONS

Searches for new physics in the form of long-lived particles have become one of the most studied objectives in the high-energy physics community in the past few years. While many BSM models predict new particles with long lifetimes, heavy neutral leptons, with the possibility to explain the non-vanishing active neutrino masses in a natural way, are perhaps among the most frequently investigated scenarios for LLPs.

In this work we have studied the sensitivity reach for GeV-scale HNLs for a recently proposed external detector at ATLAS or CMS, named ‘ANUBIS’ [1] by performing a Monte-Carlo simulation. We considered not only the minimal HNL scenario where both production and decay of the HNLs are controlled by the active-sterile neutrino mixing, but also extended theoretical scenarios: (i) a left-right symmetric model and (b) a  $U(1)_{B-L}$  model. In the minimal scenario, ANUBIS shows similar sensitivities in  $|V_{\alpha N}|^2$  ( $\alpha = e/\mu$ ) as MATHUSLA for

$m_N \lesssim 4$  GeV, but has slightly larger HNL mass reach, thanks to a larger contribution from  $W$ -boson decays. We have recast the results of the minimal scenario for HNLs produced from heavy mesons decays into the parameter space of the LRSM ( $W_R$  vs.  $m_N$ ) where both the production and decay of the HNLs proceed via an off-shell  $W_R$ , and have compared ANUBIS with other experiments. Fig. 4 shows that for  $m_N$  below the  $B$ -meson threshold, the future experiments SHiP, ANUBIS, and MATHUSLA would have the largest reach in  $m_{W_R}$ .

Finally, we estimate the exclusion limits of ANUBIS and MATHUSLA for the  $U(1)_{B-L}$  extension of the Standard Model. For the HNL production, we focus on the SM-like Higgs boson decaying into a pair of HNLs. In Fig. 5 we show that ANUBIS and MATHUSLA have similar sensitivity reaches in the plane  $|V_{\alpha N}|^2$  vs.  $m_N$ , and both may cover a large part of the parameter space corresponding to the type-I seesaw predictions based on the active neutrino masses between 0.01 eV and 0.3 eV.

We conclude that in general ANUBIS is comparable to MATHUSLA in sensitivity for probing long-lived HNLs in different models, despite its decay volume being much smaller. MATHUSLA is more sensitive to exotic physics with larger values of  $c\tau$ , as a result of its larger distance from the IP, which, however, leads only to little advantage in concrete HNL models.

### Acknowledgements

M. H. is supported by the Spanish grant FPA2017-85216-P (AEI/FEDER, UE), PROMETEO/2018/165 (Generalitat Valenciana) and the Spanish Red Consolider MultiDark FPA2017-90566-REDC. Z. S. W. is supported by the Ministry of Science, ICT & Future Planning of Korea, the Pohang City Government, and the Gyeongsangbuk-do Provincial Government through the Young Scientist Training Asia-Pacific Economic Cooperation program of APCTP.

- 
- [1] M. Bauer, O. Brandt, L. Lee, and C. Ohm, ANUBIS: Proposal to search for long-lived neutral particles in CERN service shafts, (2019), arXiv:1909.13022.
- [2] J. P. Chou, D. Curtin, and H. J. Lubatti, New Detectors to Explore the Lifetime Frontier, Phys. Lett. **B767**, 29 (2017), arXiv:1606.06298.
- [3] D. Curtin *et al.*, Long-Lived Particles at the Energy Frontier: The MATHUSLA Physics Case, Rept. Prog. Phys. **82**, 116201 (2019), arXiv:1806.07396.
- [4] J. L. Feng, I. Galon, F. Kling, and S. Trojanowski, Forward Search Experiment at the LHC, Phys. Rev. **D97**, 035001 (2018), arXiv:1708.09389.
- [5] F. Kling and S. Trojanowski, Heavy Neutral Leptons at FASER, Phys. Rev. **D97**, 095016 (2018), arXiv:1801.08947.
- [6] FASER, A. Ariga *et al.*, FASER's physics reach for long-lived particles, Phys. Rev. **D99**, 095011 (2019), arXiv:1811.12522.
- [7] V. V. Gligorov, S. Knapen, M. Papucci, and D. J. Robinson, Searching for Long-lived Particles: A Compact Detector for Exotics at LHCb, Phys. Rev. **D97**, 015023 (2018), arXiv:1708.09395.
- [8] G. Aielli *et al.*, Expression of Interest for the CODEX-b Detector, (2019), arXiv:1911.00481.
- [9] V. V. Gligorov, S. Knapen, B. Nachman, M. Papucci, and D. J. Robinson, Leveraging the ALICE/L3 cavern for long-lived particle searches, Phys. Rev. **D99**, 015023 (2019), arXiv:1810.03636.
- [10] D. Dercks, H. K. Dreiner, M. Hirsch, and Z. S. Wang, Long-Lived Fermions at AL3X, Phys. Rev. **D99**, 055020 (2019), arXiv:1811.01995.
- [11] S. Alekhin *et al.*, A facility to Search for Hidden Particles at the CERN SPS: the SHiP physics case, Rept. Prog. Phys. **79**, 124201 (2016), arXiv:1504.04855.
- [12] J. Alimena *et al.*, Searching for Long-Lived Particles beyond the Standard Model at the Large Hadron Collider, (2019), arXiv:1903.04497.
- [13] Z. S. Wang and K. Wang, Physics with Far Detectors at Future Lepton Colliders, (2019), arXiv:1911.06576.
- [14] L. Lee, C. Ohm, A. Soffer, and T.-T. Yu, Collider Searches for Long-Lived Particles Beyond the Standard Model, Prog. Part. Nucl. Phys. **106**, 210 (2019), arXiv:1810.12602.
- [15] W. Porod, M. Hirsch, J. Romao, and J. W. F. Valle, Testing neutrino mixing at future collider experiments, Phys. Rev. **D63**, 115004 (2001), arXiv:hep-ph/0011248.
- [16] P. F. de Salas, D. V. Forero, C. A. Ternes, M. Tortola, and J. W. F. Valle, Status of neutrino oscillations 2018:  $3\sigma$  hint for normal mass ordering and improved CP sensitivity, Phys. Lett. **B782**, 633 (2018), arXiv:1708.01186.
- [17] P. F. De Salas, S. Gariazzo, O. Mena, C. A. Ternes, and M. Tortola, Neutrino Mass Ordering from Oscillations and Beyond: 2018 Status and Future Prospects, Front. Astron. Space Sci. **5**, 36 (2018), arXiv:1806.11051.
- [18] P. Minkowski,  $\mu \rightarrow e\gamma$  at a Rate of One Out of  $10^9$  Muon Decays?, Phys. Lett. **B67**, 421 (1977).
- [19] T. Yanagida, Horizontal symmetry and masses of neutrinos, Conf. Proc. **C7902131**, 95 (1979).
- [20] R. N. Mohapatra and G. Senjanovic, Neutrino Mass and Spontaneous Parity Violation, Phys. Rev. Lett. **44**, 912



- (1980).
- [21] M. Gell-Mann, P. Ramond, and R. Slansky, Complex Spinors and Unified Theories, *Conf. Proc.* **C790927**, 315 (1979), arXiv:1306.4669.
- [22] J. Schechter and J. W. F. Valle, *Phys. Rev. D* **22**, 2227 (1980). doi:10.1103/PhysRevD.22.2227
- [23] R. Mohapatra and J. Valle, Neutrino Mass and Baryon Number Nonconservation in Superstring Models, *Phys. Rev.* **D34**, 1642 (1986).
- [24] R. N. Mohapatra and J. C. Pati, A Natural Left-Right Symmetry, *Phys. Rev.* **D11**, 2558 (1975).
- [25] J. C. Pati and A. Salam, Lepton Number as the Fourth Color, *Phys. Rev.* **D10**, 275 (1974), [Erratum: *Phys. Rev.* **D11**, 703(1975)].
- [26] R. N. Mohapatra and G. Senjanovic, Neutrino Masses and Mixings in Gauge Models with Spontaneous Parity Violation, *Phys. Rev.* **D23**, 165 (1981).
- [27] F. F. Deppisch, W. Liu, and M. Mitra, Long-lived Heavy Neutrinos from Higgs Decays, *JHEP* **08**, 181 (2018), arXiv:1804.04075.
- [28] F. Deppisch, S. Kulkarni, and W. Liu, Heavy neutrino production via  $Z'$  at the lifetime frontier, *Phys. Rev.* **D100**, 035005 (2019), arXiv:1905.11889.
- [29] S. Amrith *et al.*, LHC constraints on a  $B-L$  gauge model using Contur, *JHEP* **05**, 154 (2019), arXiv:1811.11452.
- [30] A. Atre, T. Han, S. Pascoli, and B. Zhang, The Search for Heavy Majorana Neutrinos, *JHEP* **05**, 030 (2009), arXiv:0901.3589.
- [31] E. J. Chun, A. Das, S. Mandal, M. Mitra and N. Sinha, *Phys. Rev. D* **100**, no. 9, 095022 (2019) doi:10.1103/PhysRevD.100.095022 [arXiv:1908.09562 [hep-ph]].
- [32] S. Mandal, M. Mitra and N. Sinha, *Phys. Rev. D* **96**, no. 3, 035023 (2017) doi:10.1103/PhysRevD.96.035023 [arXiv:1705.01932 [hep-ph]].
- [33] A. Davidson, *Phys. Rev. D* **20**, 776 (1979). doi:10.1103/PhysRevD.20.776
- [34] R. N. Mohapatra and R. E. Marshak, Local B-L Symmetry of Electroweak Interactions, Majorana Neutrinos and Neutron Oscillations, *Phys. Rev. Lett.* **44**, 1316 (1980), [Erratum: *Phys. Rev. Lett.* **44**, 1643(1980)].
- [35] E. Accomando, L. Delle Rose, S. Moretti, E. Olaiya, and C. H. Shepherd-Themistocleous, Novel SM-like Higgs decay into displaced heavy neutrino pairs in  $U(1)'$  models, *JHEP* **04**, 081 (2017), arXiv:1612.05977.
- [36] A. Das, N. Okada, S. Okada and D. Raut, *Phys. Lett. B* **797**, 134849 (2019) doi:10.1016/j.physletb.2019.134849 [arXiv:1812.11931 [hep-ph]].
- [37] A. Das, P. S. B. Dev and N. Okada, *Phys. Lett. B* **799**, 135052 (2019) doi:10.1016/j.physletb.2019.135052 [arXiv:1906.04132 [hep-ph]].
- [38] C.-W. Chiang, G. Cottin, A. Das, and S. Mandal, Displaced heavy neutrinos from  $Z'$  decays at the LHC, *JHEP* **12**, 070 (2019), arXiv:1908.09838.
- [39] CMS, A. M. Sirunyan *et al.*, Search for high-mass resonances in dilepton final states in proton-proton collisions at  $\sqrt{s} = 13$  TeV, *JHEP* **06**, 120 (2018), arXiv:1803.06292.
- [40] ATLAS, G. Aad *et al.*, Search for high-mass dilepton resonances using 139 fb<sup>-1</sup> of  $pp$  collision data collected at  $\sqrt{s} = 13$  TeV with the ATLAS detector, *Phys. Lett.* **B796**, 68 (2019), arXiv:1903.06248.
- [41] CERN Yellow Report, updated online at: <https://twiki.cern.ch/twiki/bin/view/LHCPhysics/CERNYellowReportPageBR>, Accessed: 2020-01-08.
- [42] J. C. Helo, M. Hirsch, and Z. S. Wang, Heavy neutral fermions at the high-luminosity LHC, *JHEP* **07**, 056 (2018), arXiv:1803.02212.
- [43] T. Sjostrand, S. Mrenna, and P. Z. Skands, PYTHIA 6.4 Physics and Manual, *JHEP* **05**, 026 (2006), arXiv:hep-ph/0603175.
- [44] T. Sjostrand, S. Mrenna, and P. Z. Skands, A Brief Introduction to PYTHIA 8.1, *Comput. Phys. Commun.* **178**, 852 (2008), arXiv:0710.3820.
- [45] CERN Yellow Report, updated online at: <https://twiki.cern.ch/twiki/bin/view/LHCPhysics/CERNYellowReportPageAt14TeV>, Accessed: 2020-01-08.
- [46] LHC Top WG Summary Plots, updated online at: <https://twiki.cern.ch/twiki/bin/view/LHCPhysics/LHCTopWGSummaryPlots>, Accessed: 2020-01-08.
- [47] FASER, A. Ariga *et al.*, FASER: ForWard Search Experiment at the LHC, (2019), arXiv:1901.04468.
- [48] F. F. Deppisch, P. S. Bhupal Dev, and A. Pilaftsis, Neutrinos and Collider Physics, *New J. Phys.* **17**, 075019 (2015), arXiv:1502.06541.
- [49] CHARM, F. Bergsma *et al.*, A Search for Decays of Heavy Neutrinos in the Mass Range 0.5-GeV to 2.8-GeV, *Phys. Lett.* **166B**, 473 (1986).
- [50] G. Bernardi *et al.*, FURTHER LIMITS ON HEAVY NEUTRINO COUPLINGS, *Phys. Lett.* **B203**, 332 (1988).
- [51] S. A. Baranov *et al.*, Search for heavy neutrinos at the IHEP-JINR neutrino detector, *Phys. Lett.* **B302**, 336 (1993).
- [52] DELPHI, P. Abreu *et al.*, Search for neutral heavy leptons produced in Z decays, *Z. Phys.* **C74**, 57 (1997), [Erratum: *Z. Phys.* **C75**, 580(1997)].
- [53] I. Krasnov, *Phys. Rev. D* **100**, no. 7, 075023 (2019) doi:10.1103/PhysRevD.100.075023 [arXiv:1902.06099 [hep-ph]].
- [54] M. Drewes, J. Hajer, J. Klaric, and G. Lanfranchi, NA62 sensitivity to heavy neutral leptons in the low scale seesaw model, *JHEP* **07**, 105 (2018), arXiv:1801.04207.
- [55] K. Bondarenko, A. Boyarsky, D. Gorbunov, and O. Ruchayskiy, Phenomenology of GeV-scale Heavy Neutral Leptons, *JHEP* **11**, 032 (2018), arXiv:1805.08567.
- [56] D. Curtin and M. E. Peskin, *Phys. Rev. D* **97**, no. 1, 015006 (2018) doi:10.1103/PhysRevD.97.015006 [arXiv:1705.06327 [hep-ph]].
- [57] W.-Y. Keung and G. Senjanovic, Majorana Neutrinos and the Production of the Right-handed Charged Gauge

- Boson, Phys. Rev. Lett. **50**, 1427 (1983).
- [58] D. Dercks, J. De Vries, H. K. Dreiner, and Z. S. Wang, R-parity Violation and Light Neutralinos at CODEX-b, FASER, and MATHUSLA, Phys. Rev. **D99**, 055039 (2019), arXiv:1810.03617.